Journal of Theoretical and Applied Information Technology
31st August 2024. Vol.102. No. 16

ISSN: 1992-8645 www.jatit.org E-ISSN: 1817-3195

A NEW CHANNEL ESTIMATION FRAMEWORK FOR 6G INTELLIGENT REFLECTING SURFACE-ENABLED MIMO

[1*]NAZIYA BEGUM, [2]DR. MUHIEDDIN AMER, [3]DR. OMAR ABDUL LATIF

[1*]Department of Electrical Engineering, Rochester Institute of Technology, Dubai, UAE
[2]Department of Electrical Engineering, Rochester Institute of Technology, Dubai, UAE
[3]Department of Electrical Engineering, Rochester Institute of Technology, Dubai, UAE
[1*]Corresponding Author Email Id: naziya704begum@gmail.com

ABSTRACT:

The Intelligent Reflecting Surface (IRS) serves as a technology enabling passive manipulation of wave properties like amplitude, frequency, phase, and polarization through reflection. This technology is poised to revolutionize wireless communication by enhancing spectrum and energy efficiency while demanding minimal energy consumption. However, in scenarios where an IRS assists a base station (BS) with multiple antennas and user equipment (UE) with a single antenna, obtaining Instantaneous Channel State Information (I-CSI) for every link at the IRS poses challenges due to the numerous reflective elements and passive operation of the IRS. This imposes additional burdens on the system, necessitating the integration of radio-frequency chains into the IRS system. To address this, the paper proposes a three-phase pilot-based channel estimation framework for uplink multiuser communications, utilizing modular redundancy to reduce the time needed for channel estimation. The framework leverages IRS to achieve this goal by estimating the direct channels between UEs and BSs, as well as the reflected channels between a single UEs, IRS, and BS.

Keywords: *6G, IRS, MIMO, Channel estimation, Uplink, Downlink, Power utilization*

1. INTRODUCTION

Enhancing data rates and ensuring better quality of service have been a pivotal factor in propelling advancements in wireless communication networks. The global implementation and extensive adoption of 5G wireless technology have been notable across numerous nations [1]. As a result, substantial scholarly attention has been devoted to investigating the potential of sixth-generation (6G) wireless communication, signaling a significant area of academic interest and research exploration.

6G wireless networks are envisioned to incorporate several essential characteristics, such as exceptionally high data rates, enhanced reliability, extensive global coverage, ultra-low latency, improved energy efficiency, and heightened resilience [2]. Meeting these defined criteria requires the acquisition of advanced network infrastructure and the creation of innovative approaches to enhance wireless communication. Current research emphasizes three fundamental concepts within the scope of 6G: terahertz communication, artificial intelligence, and the implementation of IRS, alternatively known as reconfigurable intelligent surfaces [3, 4]. Moreover, it is widely acknowledged that the efficiency of Multiple Input Multiple Output (MIMO) systems diminishes in environments with insufficient scattering of propagation [5]. Likewise, communication operating at millimeter-wave (mm-wave) frequencies faces challenges due to substantial path attenuation and penetration losses. These limitations have underscored the importance of creating eco-friendly and sustainable cellular networks, empowering network operators with control over the propagation environment. A new and innovative concept emerging to meet this need is called the 'smart radio environment.' This visionary concept aims to convert the wireless propagation setting into an intelligent and adaptable space actively involved in managing radio signal transmission between transmitters and receivers [6]. Integrating Intelligent Reflecting Surfaces (IRSs) within this environment is a fundamental approach to realizing this concept. These surfaces can manipulate incoming electromagnetic waves in a way that aligns with predetermined preferences. Importantly, this manipulation takes place without creating additional radio signals, thereby preventing any associated rise in power usage.

There are currently many research projects investigating various methodologies for implementing IRSs. These initiatives involve developing new meta-surfaces and reflective arrays,

promoting adaptability, setting up experiments, and confirming empirical evidence through practical testing.

In recent years, scholarly research has extensively explored the concept of IRS within the domain of wireless communication design and analysis. These studies define IRS as a flat array composed of numerous passive reflecting elements, each capable of independently controlling incident electromagnetic waves' phase to facilitate passive reflection. The intelligent adaptation and adjustment of phase shifts across the entire surface of the IRS are fundamental to achieving specific communication objectives. Known as passive beamforming or reflect beamforming [7], [8], this technique effectively realizes communication goals. Notably, recent proposals have surfaced, suggesting joint designs involving precoding at the BS and the implementation of a phase shift matrix at the IRS. These joint designs cater to diverse communication objectives. For instance, objectives range from optimizing system energy efficiency while meeting individual Signal-to-Interference-plus-Noise Ratio (SINR) constraints of users [9], to maximizing minimum user rates under a transmit power constraint [10], and minimizing transmit power at the BS while satisfying individual SINR constraints alongside maximizing total data transmission rates within power limits [11]. Earlier research has also investigated utilizing IRS to enhance minimum secrecy rates in physical layer security [12] and enabling simultaneous wireless information and power transmission [13]. Furthermore, IRS integration has been explored in wide-band Orthogonal Frequency Division Multiplexing (OFDM) and non-orthogonal multiple-access systems [14], [15], showcasing its versatility in wireless communication systems. Particularly significant within the context of sixth-generation (6G) networks [16], IRS, functioning as a dielectric meta surface, selectively reflects electromagnetic waves and addresses multipath challenges, making it well-suited for millimeter-wave or terahertz transmissions [17]. The recent surge in adopting IRS devices can be attributed to their versatility in wireless communication applications. This adoption spans various areas, including mobile edge computing, simultaneous wireless information and power transfer, improved physical layer security, device-to-device communication, mm-Wave massive MIMO, smart city applications for unmanned aerial vehicles, and intelligent IoT applications in WSN [18].

2. RELATED WORKS

The authors of [19] presented a novel concept involving a distributed Intelligent Reflecting Surface (IRS) system designed to increase the performance of millimeter-wave (mm-Wave) systems across both single-user and multi-user scenarios. This proposed system harnesses IRS technology to significantly improve the efficiency and reliability of mm-wave communication. To optimize energy efficiency while satisfying individual quality of service (QoS) criteria, the study takes on the difficulty of resource allocation.

In reference [20], the study centers around improving the accessibility and reliability of Internet of Things (IoT) services within the upcoming 6G networks by integrating Intelligent Reflecting Surfaces (IRS) into microcell deployments. The research primarily involves formulating a measurement model aimed at assessing the downlink received power in both conventional and IRS-assisted microcellular networks. This model comprises several equations specifically designed for measurement and evaluation purposes.

In [21], a huge network architecture using an Intelligent reflecting Surface (IRS) and a channel estimation technique was created. The research assessed the framework's effectiveness. The research found that by improving network coverage, the IRS installation improved end-user performance.

In reference [22], researchers investigated the use of Intelligent Reflecting Surfaces (IRS) in UAVs for wireless communication purposes. The major objective of this study was to improve spectral efficiency, communication dependability, and network coverage within the context of the Internet of Things (IoT). Stochastic capacity, symbol error rate (SER), and outage probability were the main areas of analytical equation derivation in the study. The proposed expressions were then evaluated to examine and enhance the network architecture in question.

The paper referenced as [23] examines a communication system that utilizes multiple Intelligent Reflecting Surfaces (IRSs) to establish a Massive Multiple-Input Multiple-Output (MIMO) configuration across different vehicles. The main goals involve maximizing the reflect beamforming (phase shifts) at each IRS and adjusting the transmit beamforming vectors at the transmitter. The optimization process considers SINR which is improved by either increasing the overall amplitude of the signal before the noise is introduced into it,

or by reducing the amplitude of the noise). Its goal is to maximize the minimum Quality of Service (QoS), thereby improving the overall performance of the system.

Moreover, the authors of [24] propose an adaptive cross-entropy (ACE)-based hybrid precoding approach by incorporating multi-IRS-aided systems. This hybrid precoding system utilizes machine learning techniques to optimize energy efficiency. It incorporates a small number of affordable and energy-efficient switches and inverters, resulting in enhanced energy efficiency.

A centralized design for the non-orthogonal multiple access-based multiuser beamforming (NOMA-BF) system is given in [25]. An Intelligent Reflecting Surface (IRS) is included in this design to improve system performance. During the initial phase of the optimization procedure, the active beamforming for users and the power allocation coefficient (PAC) at the transmitter are established. Subsequently, in the second stage, the passive beamforming of the Intelligent Reflecting Surface (IRS) is optimized. The overarching goal of this optimization process revolves around enhancing the network's energy efficiency (EE). However, expanding the number of sustainable users in the NOMA-BF leads to the emergence of NOMA user interference as well as inter-cluster interference (ICI).

In the investigation presented in [26], a downlink IRS)-enhanced NOMA) systems were analyzed. The research introduced a specific frequency-distance-dependent route loss model tailored for the scenario involving IRS in the NOMA downlink setup. This updated model replaced the conventional distance-based route loss model to more accurately estimate the received power and Signal-to-Interference plus Noise Ratio (SINR) in IRS-NOMA systems.

To the extent that present knowledge allows, this area lacks an appropriate channel model for IRS). This work introduces a unique method for an IRS with uplink computation that enables both the geographic growth of clusters and the mobility of transceivers and clusters. It also considers the design of reflecting coefficients based on route loss reduction. The BS steering vector is set up to make it easier for the IRS) to cooperate. Ultimately, the analytical outcomes are juxtaposed with simulation results to ascertain and validate the accuracy of this channel model.

3. PROPOSED MODEL

This section considers the scenario involving multiple-input multiple-output (MIMO) communication using an Intelligent Reflecting Surface (IRS), as shown in Figure 1. The several antennas in the BS are referred to as M_B.

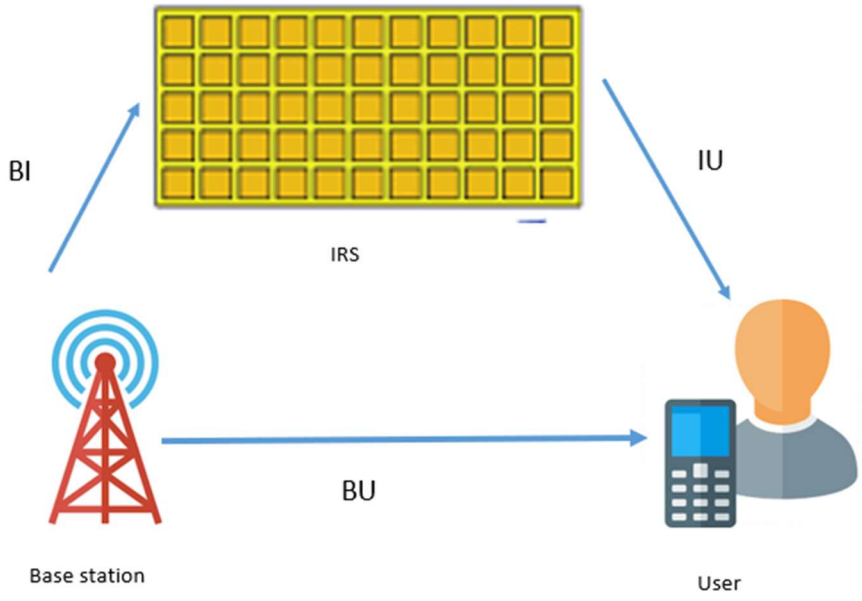

Figure 1: Architecture Of Wireless Communication Using IRS

The user has access to numerous antennas (M_U). IRS employs a multitude of passive reflecting elements (M_{XY}), calculated by multiplying M_X by M_Y to determine the total number of these elements. Here, M_X represents the quantity of items in the

horizontal direction of the IRS, while M_Y represents the quantity in the vertical direction.

Uniform linear arrays include those in BS and user. A uniform plane array might be used to describe the IRS. Every antenna element demonstrates omnidirectional properties. Three sub-channels make up this communication system: one that connects the BS to the IRS is BI; another that connects the IRS to the user is IU; and a third that connects the BS to the user is BU. The symbol H total represents the whole matrix of channel coefficients.

$$H_{total} = (H_{IU}\varphi H_{BI} + H_{BU})f \quad (1)$$

$$= \left(\sqrt{SF_{BI}SF_{IU}PL_{BIU}}h_{IU\varphi}h_{BI} + \sqrt{SF_{BU}PL_{BU}}h_{BU}\right)f \quad (2)$$

where the corresponding channel coefficient matrices are, respectively, $H_{BI} \in C^{M_{xy}\times M_B}$, $H_{IU} \in C^{M_U\times M_{xy}}$ and $H_{BU} \in C^{M_U\times M_B}$.

The channel coefficients matrices with large scale fading and without large scale fading are represented by the letters H and h, respectively. The diagonal matrix Φ, with dimensions of $M_{XY} \times M_{XY}$, represents the reflecting coefficients matrix of IRS.

The focus of this essay is on two types of large-scale fading: route loss and shadowing effect. The shadowing fading effect is modelled by the appropriate log normal random variables of the various sub-channels, SF_{BI}, SF_{BU} and SF_{IU}.

The route loss of the sub-channel between the user and the base station is indicated by PL_{BU}. The route loss of the cascaded channel with IRS assistance is denoted by PL_{BIU}. The BS steering vector is denoted by f. All of the aforementioned denotations will be calculated later.

3.1 Intelligent Reflecting Surface

IRS is related to the transmitter (Tx) and the receiver (Rx) antenna as it helps to manipulate electromagnetic waves to improve signal transmission and reception between them. To simplify the analysis of the channel model, we will concentrate on a particular system component by using IRS. The idea will be better understood by looking at an example using a transmitter (Tx) and a receiver (Rx) with a single antenna. The alignment of the peak radiation directions of the transmitting and receiving antennas with the IRS centre is a further important assumption. The results will then be extended to the case when both Tx and Rx have several antennas by using the steering vector. This will allow us to verify the proposed channel model, which assumes the provision of numerous omnidirectional antennas for both Tx and Rx. The processes of locating and recognizing objects inside IRS will be used to create a link between the IRS index and the index of the reflecting coefficients matrix. Each element's index location on the IRS is represented by the ordered pair (x, y). The number of objects along the IRS's horizontal and vertical directions are represented by the variables Mx and My, respectively. A homogeneous linear array in the context of antenna systems is a one-dimensional arrangement. The notation $r_{x,y}^t$ represents the distances between each element on IRS and Tx with a single antenna, while $r_{x,y}^r$ represents the distances between each element and RX. The IRS element intervals are denoted as δ^{l_x} and δ^{l_y} for horizontal and vertical directions, respectively. The phase of the corresponding IRS elements is represented by φ (x, y).

3.2 NOMA With Uplink

The Ref paper [26] focuses on investigating a downlink Non-Orthogonal Multiple Access (NOMA) system that was combined with an Intelligent Reflecting Surface (IRS). In this system, the BS and the UE communicate using a single antenna setup. The configuration consists of two users, identified as u_1 and u_2, located at different distances from the IRS. Specifically, u_1 is positioned closer to the IRS compared to u_2, where the distance between u_2 and the IRS is twice that of u_1. The users (u_1 and u_2) are allocated as a pair to utilize a shared frequency-time resource block. Within this framework, BS transmits a combined signal [27], represented as $x = \sqrt{\rho(a_1 s_1 + a_2 s_2)}$, where ρ denotes the transmission power of the BS, and s_1 and s_2 are the complex messages attributed to the nearby and distant users (u_1 and u_2) respectively.

The Successive Interference Cancellation (SIC) method is used by the receiver during the transmission process. The BS uses superposition coding (SC) to compensate for the lower channel characteristics of the remote user by assigning them a larger power coefficient, $a_2 > a_1$, where $a_1^2 + a_2^2 = 1$. In accordance with the Non-Orthogonal Multiple Access (NOMA) concept, the user at a distance u2 considers the message from the user close by u1 as interference when decoding its own signal s2.

Journal of Theoretical and Applied Information Technology
31st August 2024. Vol.102. No. 16

ISSN: 1992-8645 www.jatit.org E-ISSN: 1817-3195

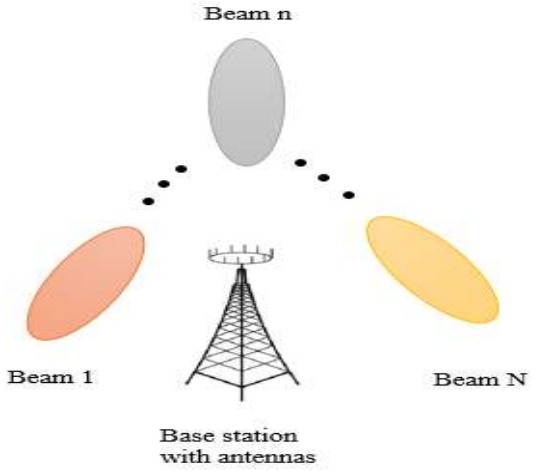

Figure 1: Architecture Of Downlink SWIPT-Assisted Cooperative NOMA

Figure 2 illustrates the architecture of the downlink system that includes Simultaneous Wireless Information and Power Transfer (SWIPT)-assisted NOMA. When user1 (u1) and user2 (u2) operate in the same frequency band, the base station (BS) can efficiently meet the needs of both users at the same time. However, in cases where there is no direct transmission path between the BS and u2 due to potential physical barriers or extensive shadowing, hindering direct communication, a cooperative relay, u1, becomes essential. u1 assists the BS in circumventing these obstacles, facilitating successful information transmission from u2 to the BS. Given the limited energy resources of u1, it initially harvests energy from the BS signal before relaying it. The channels—namely h1 from u1 to BS and h2 from u2 to BS—are characterized by Rayleigh fading properties, where *h*i = CN (0, ω_i), for iϵ {1,2}, where CN stands for complex normal variable [28].

3.3 Uplink With Dft

In this research, we simulated an uplink two-user NOMA system with an AWGN channel. To send modulated symbols, the system makes use of the Discrete Fourier Transform (DFT) method, with a root-raising cosine (RRC) pulse serving as the shaping filter.

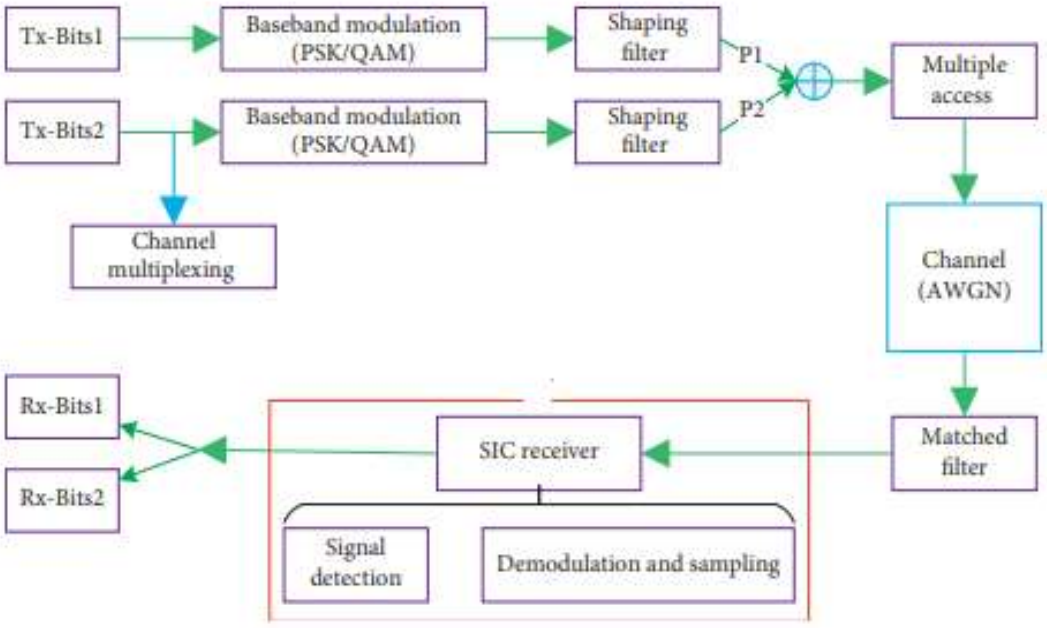

Figure 2: Workflow Of The Uplink Model With DFT

The user-generated symbols undergo shaping using the filter h(t) after the baseband modulation step. The orthogonality of the waveforms of individual symbols is lost in the time domain within the framework of the DFT. A constant α that meets the criterion $0 < \alpha < 1$ is used to denote the time parameter as αT. The representation of the single-user DFT changes significantly when evaluating a point-to-point communication system. Workflow of the uplink model with DFT are shown in the Figure 3.

$$s_i(t) = \sqrt{E_s} \sum_n a_n \, h(t - n \, \alpha T),$$

Where E_s is the energy of Binary Phase Shift Keying (BPSK) symbols, experiences influence from multiple factors. Among these factors is the Root Raised Cosine (RRC) shaping pulse, h(t), characterized by a roll-off factor of β = 0.5. Moreover, adherence to the Nyquist criterion necessitates that the symbol period, denoted as T, meets specific requirements. Each n^{th} BPSK symbol is indicated as a_n, while the compression factor of the DFT is represented by α. In scenarios where α equals 1, the entire process aligns with Nyquist transmission principles, ensuring the absence of Inter Symbol Interference (ISI).

DFT application improves spectral efficiency by bridging the spatial gap between neighbouring symbols in a constrained bandwidth. Uplink NOMA makes advantage of a combination of two users' DFT transmission symbols in the waveforms received at the BS. One type of an uplink NOMA system has a cell with two users that combine their signals in the power domain. Unlike conventional multiple access systems, these cell users share identical time and frequency resources for transmitting their signals. The premise assumes concurrent multiplexing of both users, positioning u2 at the center of the cell. It's noteworthy that the transmission power of u1 is lower than that of u2. The resultant composite DFT signal arising from the superimposition of signals from both users is outlined as follows

$$x(t) = \sum_{i=1}^{2} \sqrt{P_i s_i}\,(t) = \sum_{i=1}^{2} \sqrt{P_i} \sum_n a_n \, h(t - n \propto T)$$

User-i's transmission power is denoted by the variable Pi. SIC is a commonly used receiver technique in NOMA systems. Applying this method at user-i improves the targeted signal's SINR by reducing the impacts of multiple access interference. In certain situations, if user2's transmission signal has a higher transmission power, the SIC processing will not be activated. Instead, the base station chooses to directly detect the signal, regarding the signal from user1 as background noise. In order to decrease interference, the base station uses SIC after identifying the signal from user2. Finally, user1's signal is isolated and identified by the base station by signal detection.

4. SIMULATION ANALYSIS

Data was collected using MATLAB simulations, with a specific focus on analysing parameters such as the correlation coefficient, received power, and SINR. The system parameters were carefully examined in relation to the recommended methodology. Parameter And Values are shown in the Table 1.

Table 1: Parameter and Values

Parameter	Proposed Uplink Technique
Transmit power	6 W
Transmitter and Receiver gain	5 dB
Number of IRS transmit-receive elements	64
Length and width of the IRS elements	0.0038 m
Transmit and receive angle	45°
Reflection coefficient	0.9
Carrier frequency	90 GHz

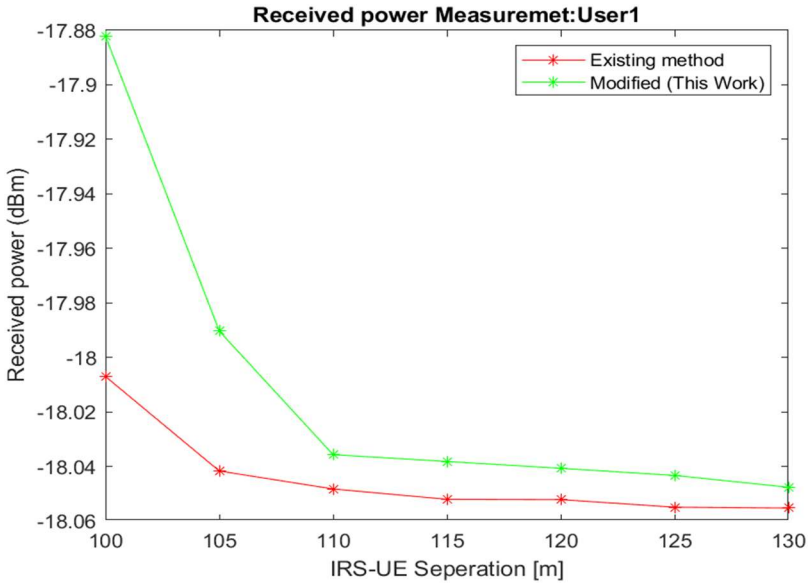

Figure 3: Calculation Of Received Power For User1

The findings of a comparison study displaying the received power for user1 are shown in Figure 4. In this research, we compare both the existing technique and the suggested approach. The receiving power in decibels (dBm) is shown by the vertical axis, while the horizontal axis shows the distance between the IRS and UE. Ensuring precise signal power measurement is crucial for evaluating the system's noise level. Upon comparison, it is clear that the received power using the recommended technique more than the received power for the existing technique. The average received power for user1 is measured at 17.99 dBm.

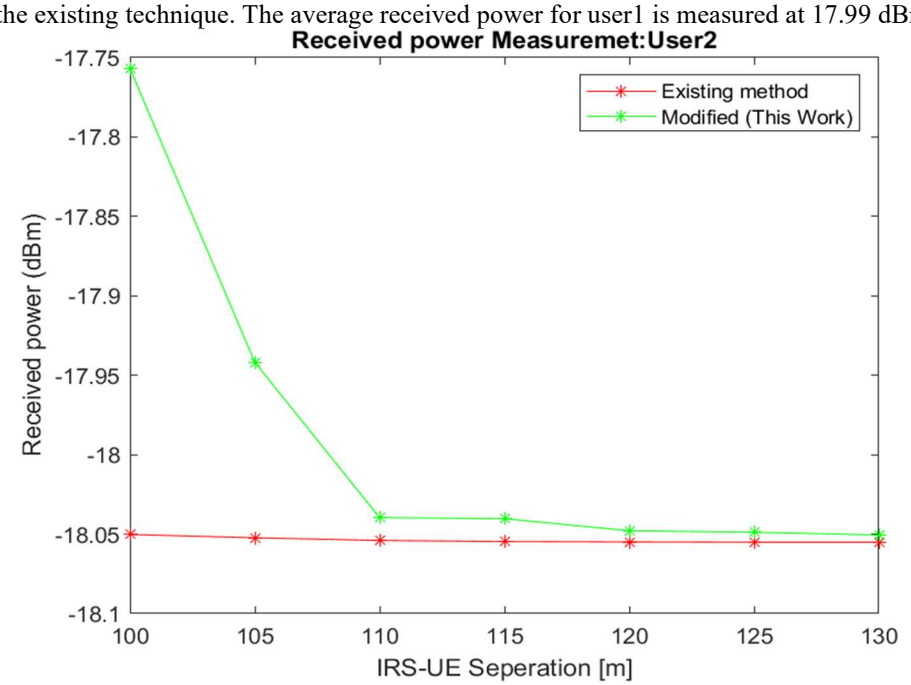

Figure 4: Calculation Of Received Power For User2

Figure 5 displays the comparative study of the received power associated with user2. This study provides a comparison between the proposed technique and the existing methodology. The y-axis displays the received power in dB, while the x-axis represents the separation of the IRS and UE. Then, evaluating the intensity of the received signal is important when considering if noise is present inside the system. A comparative analysis reveals that the recommended technique's received power is more than the existing method. User2 is receiving 17.94 dBm of mean power.

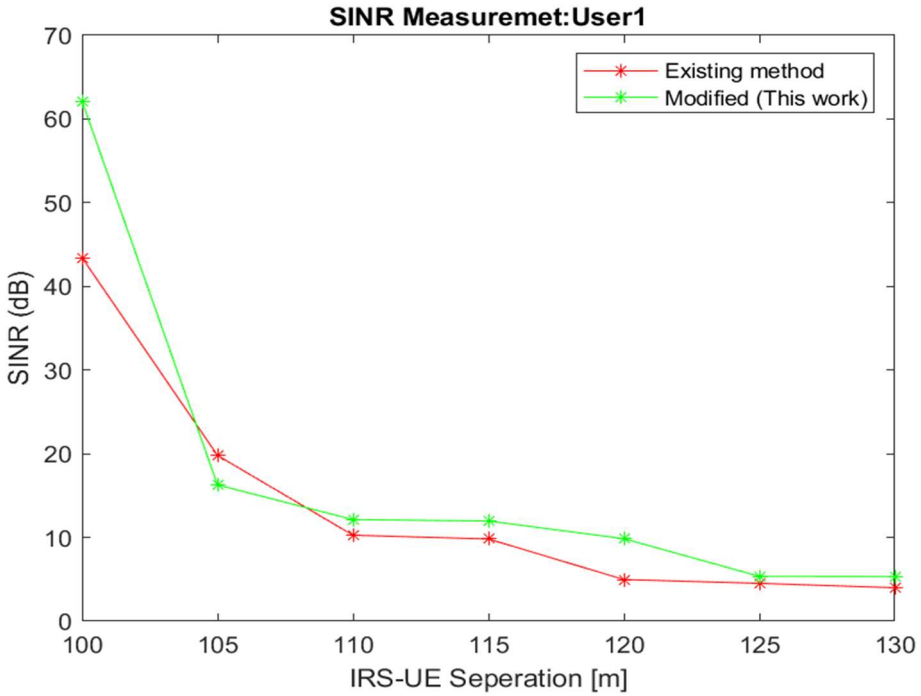

Figure 5: Calculation Of SINR For User1

The evaluation of SINR for user1 is shown in Figure 6. This research contrasts the recommended procedure with the present approach. The UE spacing is shown by the x direction, and the SINR in dB by the y direction. The measurement is related to signal quality, more precisely to the intended signal's relative strength compared to noise and unwanted interference. Upon comparison, the proposed method's SINR is determined to be 61 dB.

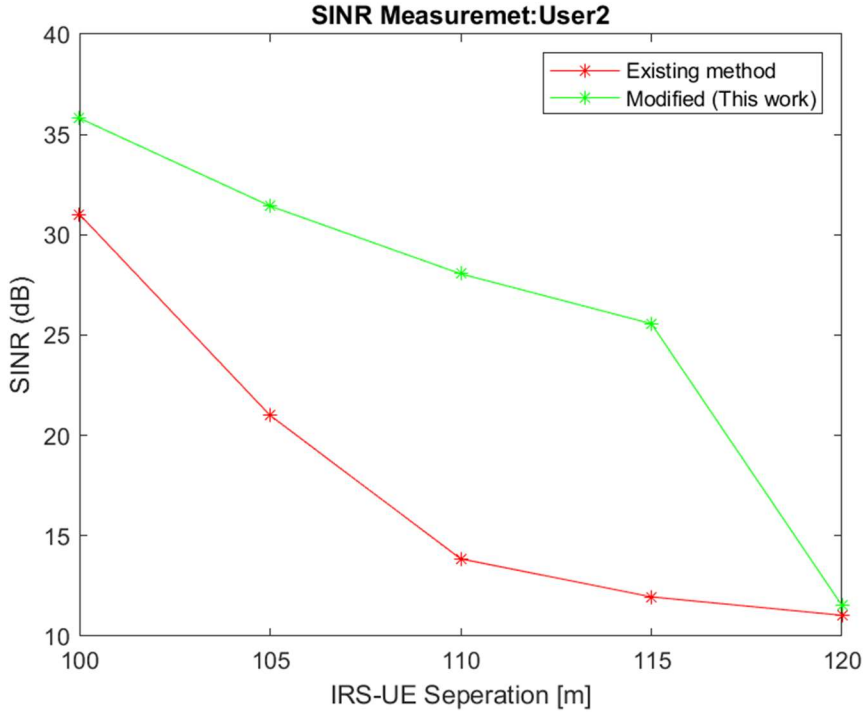

Figure 6: Calculation Of SINR For User2

The SINR comparison study, especially for user2, is shown in Figure 7. The proposed technique and the existing methodology are compared in this research. The y-axis displays the SINR in dB, while the x-axis displays the separation of the IRS and UE. The measurement is related to signal quality, more precisely to the intended signal's relative strength compared to noise and unwanted interference. The recommended technique's SINR is observed to be 36 dB upon comparison.

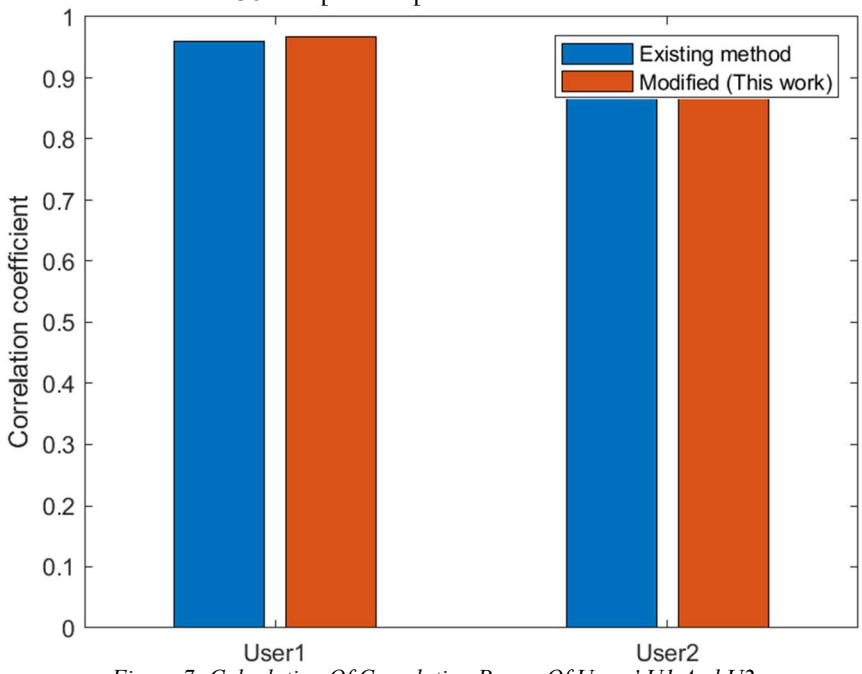

Figure 7: Calculation Of Correlation Power Of Users' U1 And U2

Figure 8 displays the correlation power evaluation of user's u1 and u2. The proposed technique and the existing strategy are compared in this research. The y-axis denotes the correlation coefficient, while the x-axis denotes the distance between the IRS and UE. A statistical measure used to quantify the degree of linearity between two variables is the correlation coefficient. This variable may have values somewhere between -1 and 1. The comparison reveals that the recommended method has a smaller correlation coefficient. Summary Of Results are shown in the Table 2.

Table 2: Summary Of Results

Parameter	Proposed Uplink Method	Existing Uplink Method
Mean Received Power (user1)	17.99 dBm	11.52 dBm
Mean Received Power (user2)	17.94 dBm	12.48 dBm
Mean SINR (user1)	16 dB	10 dB
Mean SINR (user2)	31 dB	13 dB
Correlation Coefficient (u1 & u2)	Lower	Higher

The proposed technique for channel estimation in IRS-enabled wireless communication systems presents promising results. Mean received power for both users u1 and u2 is slightly higher compared to the existing technique. Additionally, the mean SINR significantly improves, with values of 16 dB for user 1 and 31 dB for user2. Moreover, the proposed technique exhibits a lower correlation coefficient, indicating enhanced system robustness. These findings collectively suggest that the proposed technique enhances signal quality and system performance compared to existing methods, making it a promising approach for practical

implementation in real-world wireless communication systems.

5. CONCLUSION

The need for a channel estimation method that can handle the massive surge in wireless data traffic is on the rise. The widespread use of large multiple-input multiple-output (MIMO) wireless access networks is rapidly being acknowledged as a viable option for meeting the demands of the current broadband communication requirements. This technology utilizes antennas at both the transmitting and receiving ends to enhance spectrum and energy efficiency through simple processing techniques. The proposed framework aims to determine the minimum pilot sequence length needed for accurate channel estimation at the base station in less noise conditions. In addition, channel estimators are developed for scenarios involving noise at the BS. We have provided simulation results to illustrate the effectiveness of our framework. These examples demonstrate a comparison between the proposed approach and a standard technique that does not consider channel correlation.

CONFLICTS OF INTEREST

The authors declare no conflicts of interest.

DATA AVAILABILITY STATEMENT

Not Applicable

REFERENCES

[1] Wild, T.; Braun, V.; Viswanathan, H. Joint Design of Communication and Sensing for Beyond 5G and 6G Systems. *IEEE Access* 2021, *9*, 30845–30857.

[2] Rajatheva, N.; Atzeni, I.; Bicais, S.; Bjornson, E.; Bourdoux, A.; Buzzi, S.; D'Andrea, C.; Dore, J.B.; Erkucuk, S.; Fuentes, M.; et al. Scoring the terabit/s goal: Broadband connectivity in 6G. *arXiv* 2020, arXiv:2008.07220.

[3] Dang, S.; Amin, O.; Shihada, B.; Alouini, M.S. What should 6G be? *Nat. Electron.* 2020, *3*, 20–29.

[4] Viswanathan, H.; Mogensen, P.E. Communications in the 6G era. *IEEE Access* 2020, *8*, 57063–57074.

[5] Q. U.-A. Nadeem, A. Kammoun, M. Debbah, and M.-S. Alouini, "Asymptotic analysis of RZF over double scattering channels with MMSE estimation," IEEE Trans. Wireless Commun., vol. 18, no. 5, pp. 2509–2526, May 2019.

[6] M. D. Renzo et al., "Smart radio environments empowered by reconfigurable AI meta-surfaces: An idea whose time has come," EURASIP J. Wireless Commun. Netw., vol. 2019, p. 129, Dec. 2019

[7] Q. Wu and R. Zhang, "Intelligent reflecting surface enhanced wireless network: Joint active and passive beamforming design," in Proc. IEEE Global Commun. Conf. (GLOBECOM), Dec. 2018, pp. 1–6.

[8] Q. Wu and R. Zhang, "Intelligent reflecting surface enhanced wireless network via joint active and passive beamforming," IEEE Trans. Wireless Commun., vol. 18, no. 11, pp. 5394–5409, Nov. 2019.

[9] C. Huang, A. Zappone, G. C. Alexandropoulos, M. Debbah, and C. Yuen, "Reconfigurable intelligent surfaces for energy efficiency in wireless communication," IEEE Trans. Wireless Commun., vol. 18, no. 8, pp. 4157–4170, Aug. 2019.

[10] Q. U.-A. Nadeem, A. Kammoun, A. Chaaban, M. Debbah, and M.-S. Alouini, "Asymptotic Max-Min SINR analysis of reconfigurable intelligent surface assisted MISO systems," IEEE Trans. Wireless Commun., early access, Apr. 14, 2020, doi: 10.1109/TWC.2020.2986438.

[11] C. Pan et al., "Multicell MIMO communications relying on intelligent reflecting surface," Jul. 2019. [Online]. Available: arXiv:1907.10864.

[12] H. Guo, Y.-C. Liang, J. Chen, and E. G. Larsson, "Weighted sum-rate maximization for reconfigurable intelligent surface aided wireless networks," IEEE Trans. Wireless Commun., vol. 19, no. 5, pp. 3064–3076, May 2020.

[13] J. Chen, Y.-C. Liang, Y. Pei, and H. Guo, "Intelligent reflecting surface: A programmable wireless environment for physical layer security," IEEE Access, vol. 7, pp. 82599–82612, 2019. [20] Q. Wu and R. Zhang, "Weighted sum power maximization for intelligent reflecting surface aided SWIPT," IEEE Wireless Commun. Lett., vol. 9, no. 5, pp. 586–590, May 2020.

[14] Y. Yang, S. Zhang, and R. Zhang, "IRS-enhanced OFDM: Power allocation and passive array optimization," May 2019. [Online]. Available: arXiv:1905.00604.

[15] B. Zheng, Q. Wu, and R. Zhang, "Intelligent reflecting surface-assisted multiple access with user pairing: NOMA or OMA?" IEEE Commun. Lett., vol. 24, no. 4, pp. 753–757, Apr. 2020

[16] Chen, Z.; Ning, B.; Han, C.; Tian, Z.; Li, S. Intelligent Reflecting Surface Assisted Terahertz Communications Toward 6G. *IEEE Wirel. Commun.* 2021, *28*, 110–117.

[17] Chen, Z.; Tang, J.; Zhang, X.Y.; So, D.K.C.; Jin, S.; Wong, K.K. Hybrid evolutionary-based sparse channel estimation for IRS-assisted mmWave MIMO systems. *IEEE Trans. Wirel. Commun.* 2021, *21*, 1586–1601.

[18] Liu, Y.; Liu, X.; Mu, X.; Hou, T.; Xu, J.; Di Renzo, M.; Al-Dhahir, N. Reconfigurable intelligent surfaces: Principles and opportunities. *IEEE Commun. Surv. Tutor.* 2021, *23*, 1546–1577

[19] Khorasgani, A. Q., Tabataba, F. S., Soorki, M. N., & Fazel, M. S. (2023). Energy-Efficient Resource Allocation for Multi-IRS-Aided Indoor 6G Networks. *arXiv preprint arXiv:2302.06865*.

[20] Mahbub, M., & Shubair, R. M. (2023). Downlink Received Power Performance Analysis of IRS for 6G Networks. *arXiv preprint arXiv:2305.03174*.

[21] 60. G. Yu, X. Chen, C. Zhong, H. Lin and Z. Zhang, "Large Intelligent Reflecting Surface Enhanced Massive Access for B5G Cellular Internet of Things," 2020 IEEE 91st Vehicular Technology Conference (VTC2020-Spring), 2020, pp. 1-5.

[22] A Mahmoud, S. Muhaidat, P. C. Sofotasios, I. Abualhaol, O. A. Dobre and H. Yanikomeroglu, "Intelligent Reflecting Surfaces Assisted UAV Communications for IoT Networks: Performance Analysis," in IEEE Transactions on Green Communications and Networking, vol. 5, no. 3, pp. 1029-1040, Sept. 2021.

[23] Shabir, M. W., Nguyen, T. N., Mirza, J., Ali, B., & Javed, M. A. (2022). Transmit and Reflect Beamforming for Max-Min SINR in IRS-Aided MIMO Vehicular Networks. *IEEE Transactions on Intelligent Transportation Systems*.

[24] Elganimi, T. Y., & Rabie, K. M. (2022, April). Multi-IRS-aided millimeter-wave massive MIMO with energy-efficient hybrid precoding schemes. In *2022 IEEE Wireless Communications and Networking Conference (WCNC)* (pp. 1075-1080). IEEE.

[25] Ihsan, A., Chen, W., Asif, M., Khan, W. U., Wu, Q., & Li, J. (2022). Energy-efficient IRS-aided NOMA beamforming for 6G wireless communications. *IEEE Transactions on Green Communications and Networking*, *6*(4), 1945-1956.

[26] Mahbub, Mobasshir, and Raed M. Shubair. "Investigation of the Intelligent Reflecting Surfaces-Assisted Non-Orthogonal Multiple Access in 6G Networks." In 2022 IEEE 13th Annual Information Technology, Electronics and Mobile Communication Conference (IEMCON), pp. 0492-0496. IEEE, 2022.

[27] Cheng, Y., Li, K. H., Liu, Y., Teh, K. C., & Poor, H. V. (2021). Downlink and uplink intelligent reflecting surface aided networks: NOMA and OMA. IEEE Transactions on Wireless Communications, 20(6), 3988-4000.

[28] Björnson, E., & Sanguinetti, L. (2020). Rayleigh fading modeling and channel hardening for reconfigurable intelligent surfaces. IEEE Wireless Communications Letters, 10(4), 830-83